REPORT DOCUMENTATION PAGE

Form Approved
OMB No. 0704-0188

1. AGENCY USE ONLY (Leave blank)	2. REPORT DATE	3. REPORT TYPE AND DATES COVERED
	30 October 1996	Technical

4. TITLE AND SUBTITLE

FORMATION, STRUCTURAL CHARACTERIZATION, AND THERMAL DECOMPOSITION OF THE ADDUCTS, $X_3Ga{\bullet}P(TMS)_3$ [X = Cl, Br, I]

5. FUNDING NUMBERS

•N00014-95-1-0194
R&T Project 3135008---16
•Dr. Harold E. Guard

6. AUTHOR(S)

J. F. Janik, R. A. Baldwin, R. L. Wells, W. T. Pennington, G. L. Schimek, A. L. Rheingold, L. M. Liable-Sands

7. PERFORMING ORGANIZATION NAME(S) AND ADDRESS(ES)

Department of Chemistry
Duke University
Durham, NC 27708-0346

8. PERFORMING ORGANIZATION REPORT NUMBER

Technical Report
No. DU/DC/TR-63

9. SPONSORING / MONITORING AGENCY NAME(S) AND ADDRESS(ES)

Office of Naval Research
300 North Quincy Street
Arlington, VA 22217-5000

10. SPONSORING / MONITORING AGENCY REPORT NUMBER

11. SUPPLEMENTARY NOTES

Accepted for publication in *Organometallics*

12a. DISTRIBUTION / AVAILABILITY STATEMENT

Approved for Public Release
Distribution Unlimited

12b. DISTRIBUTION CODE

13. ABSTRACT (Maximum 200 words)

The adducts, $X_3Ga{\bullet}P(TMS)_3$ [X = Cl (**1**), Br (**2**), I (**3**)], were prepared in high yields from the combination of the respective gallium trihalides with $P(TMS)_3$ in hydrocarbon solvents at ambient temperature. The adducts were characterized by NMR, MS, elemental analysis, and single-crystal X-ray structure determinations. Particularly, the ^1H NMR study of 1-3 helped correct our previously published results regarding momomer-dimer equilibria of the related $[X_2GaP(SiMe_3)_2]_2$ in solution. The crystal structure determinations showed that 1 and 2 were solvated, $1{\bullet}C_6H_5Cl$ and $2{\bullet}C_7H_8$, respectively, and that 3 was solvent-free. The thermal decomposition behavior of **1-3** was studied by TGA along with a determination of the volatiles from pyrolysis and analysis of the final solid product. The pyrolyses of **1-3** at 450 °C under vacuum resulted in nanocrystalline GaP with 4-5 nm particle average sizes as determined by X-ray powder diffraction (XRD) and, for pyrolysis of **2**, by transmission electron microscopy (TEM); in addition, small quantities of amorphous S/C/H containing phases were also formed.

14. SUBJECT TERMS

gallium phosphide, nanocrystalline, adducts, structure

15. NUMBER OF PAGES

21

16. PRICE CODE

17. SECURITY CLASSIFICATION OF REPORT	18. SECURITY CLASSIFICATION OF THIS PAGE	19. SECURITY CLASSIFICATION OF ABSTRACT	20. LIMITATION OF ABSTRACT
Unclassified	Unclassified	Unclassified	Unlimited

OFFICE OF NAVAL RESEARCH

Grant N00014-95-1-0194
R&T Project 3135008---16

Dr. Harold E. Guard

Technical Report No. DU/DC/TR-63

FORMATION, STRUCTURAL CHARACTERIZATION, AND THERMAL DECOMPOSITION OF THE ADDUCTS, $X_3Ga{\cdot}P(TMS)_3$ [X = Cl, Br, I]

Jerzy F. Janik,[1] Ryan A. Baldwin,[1] Richard L. Wells,[1]
William T. Pennington,[2] George L. Schimek,[2]
Arnold L. Rheingold,[3] and Louise M. Liable-Sands[3]

[1]Department of Chemistry, Duke University, Durham, NC 27708
Department of Chemistry, Clemson University, Clemson, SC 29634
[3]Department of Chemistry, University of Delaware, Newark, DE 19716

Accepted for publication in *Organometallics*

Duke University
Department of Chemistry,
P. M. Gross Chemical Laboratory
Box 90346
Durham, NC 27708-0346

30 October 1996

Formation, Structural Characterization, and Thermal Decomposition of the Adducts $X_3Ga{\cdot}P(SiMe_3)_3$ [X = Cl, Br, I].

Jerzy F. Janik†, Ryan A. Baldwin, and Richard L. Wells*
Department of Chemistry, Paul M. Gross Chemical Laboratory, Duke University
Durham, NC 27708-0346

William T. Pennington and George L. Schimek
Department of Chemistry, H. L. Hunter Chemical Laboratory, Clemson University,
Clemson, South Carolina 29634

Arnold L. Rheingold and Louise M. Liable-Sands
Department of Chemistry, Drake Hall, University of Delaware, Newark, Delaware 19716

The adducts, $X_3Ga{\cdot}P(SiMe_3)_3$ [X = Cl (**1**), Br (**2**), I (**3**)], were prepared in high yields from the combination of the respective gallium trihalides with $P(SiMe_3)_3$ in hydrocarbon solvents at ambient temperature. The adducts were characterized by NMR, MS, elemental analysis, and single-crystal X-ray structure determinations. Particularly, the ^1H NMR study of **1-3** helped to correct our previously published results regarding monomer-dimer equilibria of the related $[X_2GaP(SiMe_3)_2]_2$ in solution. The crystal structure determinations showed that **1** and **2** were solvated, **1**·C_6H_5Cl and **2**·C_7H_8, respectively, and that **3** was solvent-free. The thermal decomposition of **1-3** was studied by TGA along with a determination of the volatiles from pyrolysis and analysis of the final solid product. The pyrolyses of **1-3** at 450 °C under vacuum resulted mainly in nanocrystalline GaP with 4-5 nm particle average sizes as determined by X-ray powder diffraction (XRD) and, for pyrolysis of **2**, by transmission electron microscopy (TEM); in addition, small quantities of amorphous Si/C/H containing phases were also formed.

---

* Correspondence to: R. L. Wells

† On leave from the University of Mining and Metallurgy, Krakow, Poland

Introduction

The pool of 13-15 single-source precursors for solid-state materials usually includes simple Lewis acid-base adducts of the type $X_3A(13)\cdot B(15)Y_3$ (X, Y - leaving groups) or their available elimination-condensation products, such as the related oligomeric $[X_2ABY_2]_n$.[1] Ideally, subsequent thermal decomposition of these precursors would result in clean, complete elimination of the easily removable XY, sometimes with assisted β-hydride elimination processes, and condensation of the AB solid network. It is desired that the expected high driving force for elimination-condensation reactions in suitable systems will yield the solid product at significantly lower temperatures than traditional syntheses from elements or oxides and, thus, enable better control over materials forms, product purity, and crystallinity. In this approach, adducts have the advantage over oligomeric compounds in that they are usually prepared in a straightforward way and in almost stoichiometric yields. However, this property may often be offset by more complex thermal decomposition pathways that can result in cracking side-reactions of amenable ligands and formation of additional solid phases to AB. Indeed, this seems to be a common feature for most precursors utilized in bulk syntheses and, in numerous cases, it has hindered the development of high purity 13-15 materials.[2] On the other hand, the resulting nanocrystalline composite materials may themselves find new applications due to their unique properties and be the source of pure 13-15 phases if appropriate separation methods are developed.

Our previous investigations of the synthetic routes to nanocrystalline GaP and GaAs resulted in the implementation of two independent methods. First, the metathetical reactions between $(Na/K)_3E$ (E = P, As) and gallium trihalide solutions in refluxing coordinating solvents afforded the respective GaP and GaAs nanocrystalline materials.[3] Second, we prepared and structurally characterized the dimeric elimination-condensation products, $[X_2GaP(SiMe_3)_2]_2$ (X = Cl,[4] Br,[5a] I[5a,b]), all of which yielded crystalline, nanosized GaP as the major product upon pyrolysis in the 400-500 °C range.

A closer examination of the properties of the $X_3Ga + P(SiMe_3)_3$ (X = Cl, Br, I) reaction systems under different conditions has led us to the isolation of the respective Lewis acid-base adducts, $X_3Ga\cdot P(SiMe_3)_3$ [X = Cl(**1**), Br(**2**), I(**3**)], in high yields. We report herein the preparation, characterization (including crystal structure determinations), and thermal decomposition of these adducts.

Experimental Section

General techniques. All experiments were performed using standard vacuum/Schlenk techniques.[6] Hydrocarbon solvents were distilled from Na benzophenone ketyl or Na/K alloy prior to use. Chlorobenzene was dried over P_2O_5. Anhydrous $GaCl_3$ (99.999%), $GaBr_3$ (99.999%) were purchased from Strem Chemicals while GaI_3 (99.999%) was obtained from Alfa/Johnson-Matthey; all were used as received. $P(SiMe_3)_3$ was prepared by a literature method.[7] ^1H, $^{13}C\{^1H\}$, and ^{31}P NMR spectra were recorded on a Varian Unity 400 spectrometer at 25 °C from saturated d_8-toluene or d-chloroform solutions, and referenced by generally accepted methods. Mass spectra were collected on a JEOL JMS-SX 102A spectrometer operating in the electron ionization mode at 20 eV; the assignment of the ion fragments was supported by comparisons with theoretical ion distributions. IR spectra of solids and gaseous pyrolysis products were acquired using KBr pellets and a gas cell, respectively, on a BOMEM Michelson MB-100 FT-IR spectrometer. A calibrated manifold was used for volume estimations of reaction gases. TGA/DTA analyses were acquired under nitrogen flow on a TA Instruments SDT 2960 simultaneous TGA/DTA apparatus. Elemental analyses were provided by E + R Microanalytical Laboratory, Corona, NY. Melting points (uncorrected) were determined with a Thomas-Hoover Uni-melt apparatus for samples flame-sealed in glass capillaries. Single-crystal X-ray diffraction studies were performed for **1**•C_6H_5Cl and **2**•C_7H_8 at Clemson University, Clemson, SC, on a Rigaku AFC7R diffractometer using graphite-monochromated Mo Kα radiation (λ = 0.71073 Å). Single-crystal X-ray diffraction study for **3** was carried out at the University of Delaware, Newark, DE, on a Siemens P4 diffractometer utilizing graphite-monochromated Mo Kα radiation (λ = 0.71073 Å). HRTEM microscopy was performed at the Analytical Instrumental Facility of North Carolina State University on a Topcon EM002B instrument using a 200 kV accelerating voltage. Magnifications used to derive the distance between lattice fringes were calibrated using high resolution TEM images of Si. XRD data were collected using mineral oil coated samples on a Phillips XRD 3000 diffractometer utilizing Cu Kα radiation; the average particle size was calculated using the Scherrer equation applied to the (111) diffraction line of cubic GaP.

Synthesis of Cl_3Ga•$P(SiMe_3)_3$ (1). 0.35 g (2.0 mmol) of $GaCl_3$ was dissolved in 30 mL of hexane or pentane in a 100 mL Schlenk flask. To this solution, 30 mL of a hexane solution of $P(SiMe_3)_3$ (0.50 g or 2.0 mmol) was slowly added with stirring at room temperature. An instantaneous formation of a white precipitate was observed. After overnight stirring, the volatiles were removed in vacuo to yield **1** as a white, powdery

solid: 0.80 g, yield 94%. **1** is sparingly soluble in hexane and only slightly soluble in toluene, chlorobenzene, and chloroform. X-ray quality crystals of **1** were grown from chlorobenzene at -30 °C. Melting behavior: beginning at 130 °C, gradual change of color from white through yellow to bright brown; no melting to 300 °C. Anal. Found (calcd) for $C_9H_{27}Cl_3GaPSi_3$: C, 25.33 (25.34); H, 6.20 (6.38). ^1H NMR (d_8-toluene): δ 0.29 (d, J_{P-H} = 6.2 Hz); ^1H NMR (d-chloroform): δ 0.59 (d, J_{P-H} = 6.3 Hz). $^{13}C\{^1H\}$ NMR (d_8-toluene): δ 1.8 (d, J_{P-C} = 8.4 Hz); ^{13}C NMR (d-chloroform): δ 2.2 (d, J_{P-C} = 8.4 Hz). Due to low solubility, no unequivocal ^{31}P NMR resonance was discernible after several thousand scans. MS: m/e (intensity)(ion): peak clusters around: 411 (1)($Cl_3Ga{\bullet}P(SiMe_3)_3$-Me, M^+-Me), 391 (11)(M^+-Cl), 303 (3)(M^+-Me_3SiCl-Me), 283 (3)(M^+-Me_3SiCl-Cl), 250 (100)($P(SiMe_3)_3$), 235 (22)($P(SiMe_3)_3$-Me), 177 (1)($P(SiMe_3)_2$), 176 (2)($GaCl_3$), 162 (10)($P(SiMe_3)_2$-Me), 147 (5)($P(SiMe_3)_2$-2Me), 141 (4)($GaCl_2$), 108 (3)(Me_3SiCl), 95 (9)(PSi_2H_8), 73 (9)($SiMe_3$).

Thermal decomposition of 1.

(a) Thermogravimetric changes. Curve **A** in Figure 1 shows the weight changes of **1** under nitrogen flow and 5 °C/min heating rate: stage 1 (from 30 to 80 °C), weight loss of 27%; stage 2 (from 80 to 130 °C), weight loss of 26% ; stage 3 (from 130 to 500 °C), weight loss of 8%. Total observed weight loss = 61%. Calculated weight loss for $Cl_3Ga{\bullet}P(SiMe_3)_3$ = GaP + 3 Me_3SiCl, 76.4%.

(b) Pyrolysis at 450 °C under vacuum. 0.15 g (0.35 mmol) of **1** was placed in a sublimator that was attached to a -196 °C cold trap. The system was then evacuated, closed under vacuum, and the sublimator was heated at 100 °C (0.5 h), 150 °C (0.5 h), 200 °C (0.5 h), and 450 °C (12 h). In the 150-200 °C range, particle dusting was observed due to extensive gas evolution. The final products consisted of a brown powdery solid (0.025 g), some white solid on colder parts, and condensable and non-condensable volatiles. Non-condensable (CH_4), approx. 0.10 mmol; condensable (Me_3SiCl), 0.85 mmol. Elemental analysis for solid product: Ga, 64.52; P, 28.44; C, 4.47 (Σ 97.43); Ga/P ratio, 1.01/1.00. An X-ray diffraction pattern was obtained for the solid product from a parallel, 1 mmol scale pyrolysis performed at 450 °C with a continuous removal of volatiles. The spectrum matched the pattern for cubic GaP (JCPDS file 12-191) and a 5.0 nm average particle size was calculated using the Scherrer equation.

Synthesis of $Br_3Ga{\bullet}P(SiMe_3)_3$ (2). The preparation of **2** was carried out in a manner similar to that of **1**. Quantities of reagents: $GaBr_3$, 0.93 g (3.0 mmol); $P(SiMe_3)_3$, 0.75 g (3.0 mmol). Yield of **2**, 1.52 g or 90%. The solubility of **2** in common solvents is

rather low but it is better than that of **1**. X-ray quality crystals were obtained from a toluene solution of **2** at -30 °C. Melting behavior: beginning at 150 °C, color changed from white through yellow to brown; no melting to 300 °C. Anal. Found (calcd) for $C_9H_{27}Br_3GaPSi_3$: C, 19.10 (19.30); H, 4.86 (4.86). ^1H NMR (d_8-toluene): δ 0.32 (d, J_{P-H} = 6.2 Hz). $^{13}C\{^1H\}$ NMR (d_8-toluene): δ 2.0 (d, J_{P-C} = 7.6 Hz). Due to low solubility, no unequivocal ^{31}P NMR resonance was obtained after several thousand scans. MS: m/e (intensity)(ion): peak clusters around: 623 (4)($[Br_2GaP(SiMe_3)_2]_2$-2$SiMe_3$-3Me; also some contribution from Ga_2Br_6 at m/e 620), 479 (12)($Br_3GaP(SiMe_3)_3$-Br, M^+-Br), 391 (2)(M^+-Me_3SiBr-Me), 377 (3)(M^+-Me_3SiBr-2Me), 327 (6)(), 313 (9)($Br_2GaP(SiMe_3)_2$-Br-Me), 309 (4)($GaBr_3$), 250 (100)($P(SiMe_3)_3$), 235 (23)($P(SiMe_3)_3$-Me), 229 (8)($GaBr_2$), 177 (2)($P(SiMe_3)_2$), 162 (15)($P(SiMe_3)_2$-Me), 154 (22)(Me_3SiBr), 147 (9)($P(SiMe_3)_2$-2Me), 139 (69)(Me_3SiBr-Me), 73 (44)($SiMe_3$).

Thermal decomposition of 2.

(a) Thermogravimetric changes. Curve **B** in Figure 1 displays the weight changes of **2** under nitrogen flow and 5 °C/min heating rate: stage 1 (from 30 to 110 °C), weight loss of 24%; stage 2 (from 110 to 190 °C), weight loss of 38%; stage 3 (from 190 to 500 °C), weight loss of 14%. Total observed weight loss = 76%. Theoretical weight loss for $Br_3Ga{\bullet}P(SiMe_3)_3$ = GaP + 3 Me_3SiBr, 82.0%.

(b) Pyrolysis at 450 °C under vacuum. 0.50 g (0.89 mmol) of **2** was placed in a sublimator that was attached to a -196 °C cold trap. The system was then evacuated, closed under vacuum, and the sublimator was heated at 100 °C (0.5 h), 150 °C (0.5 h), 200 °C (0.5 h), and 450 °C (12 h). The recovered product was a dark brown solid, 0.08 g. Some yellowish solid was also deposited on the colder parts of the set-up. Non-condensable volatiles (CH_4), 0.30 mmol; condensable volatiles (Me_3SiBr), 1.80 mmol. Elemental analysis for solid product: Ga, 58.17; P, 27.63; C, 0.73 (Σ 86.53); Ga/P ratio, 0.94/1.00. IR (cm^{-1}): 809 (w, br), 1077 (s, br). An X-ray diffraction pattern for the product matched the pattern for cubic GaP (JCPDS file 12-191) and a 4.6 nm average particle size was calculated using the Scherrer equation. A TEM micrograph obtained for the solid is shown in Figure 2.

Synthesis of $I_3Ga{\bullet}P(SiMe_3)_3$ (3). The preparation of **3** was performed similarly as the preparation of **1**, except for the isolation of crystals for structure determination (vide infra). Quantities of reagents: GaI_3, 0.45 g (1.0 mmol); $P(SiMe_3)_3$, 0.25 g (1.0 mmol). Yield of **3**, 0.61 g or 87%. The solubility of **3** in common solvents is similar to that of **2**. X-ray quality crystals of **3** were fortuitously obtained as the only identifiable product from

a reaction mixture containing GaI_3, $P(SiMe_3)_3$, and $Sb(SiMe_3)_3$ that was stored at -30 °C for several days. The melting behavior of **3** closely paralleled that of **1** and **2**. Anal. Found (calcd) for $C_9H_{27}I_3GaPSi_3$: C, 3.13 (3.88), H, 12.66 (15.42). The low C and H contents are thought to result from analytical complications due to the thermal instability of **3**. ^1H NMR (d_8-toluene): δ 0.38 (d, J_{P-H} = 5.6 Hz). $^{13}C\{^1H\}$ NMR (d_8-toluene): δ 2.3 (d, J_{P-C} = 7.2 Hz). Due to low solubility, no unequivocal ^{31}P NMR resonance was recorded after several thousand scans. MS: m/e (intensity)(ion): peak clusters around: 698 (2)($I_3Ga_2PSi_2C_6H_{18}$), 573 (33)($I_2GaPSi_3C_9H_{27}$, M^+-I), 450 (57)(GaI_3), 373 (6)(M^+-Me_3SiI-I), 323 (54)(GaI_2), 250 (100)($P(SiMe_3)_3$), 235 (25)($P(SiMe_3)_3$-Me), 220 (7)($P(SiMe_3)_3$-2Me), 200 (28)($P(SiMe_3)_3$-3Me-5H), 196 (7)(GaI), 185 (13)($P(SiMe_3)_3$-4Me-5H), 163 (11)($P(SiMe_3)_3$-$SiMe_3$-Me+H), 148 (10)($P(SiMe_3)_3$-$SiMe_3$-2Me+H), 75 (53)($PSiCH_4$), 71(1)(PSiC).

Thermal decomposition of 3.

(a) Thermogravimetric changes. Curve **C** in Figure 1 displays the weight changes of **3** under nitrogen flow and 5 °C/min heating rate: stage 1 (from 30 to 150 °C), weight loss of 28%; stage 2 (from 150 to 230 °C), weight loss of 30%; stage 3 (from 230 to 500 °C), weight loss of 24%. Total observed weight loss = 82%. Theoretical weight loss for $I_3Ga{\cdot}P(SiMe_3)_3$ = GaP + 3 Me_3SiI, 85.6%.

(b) Pyrolysis at 450 °C under vacuum. 0.55 g (0.79 mmol) of **3** was placed in a sublimator that was attached to a -196 °C operating cold trap. The system was evacuated, closed under vacuum, and the sublimator was heated at 150 °C (0.5 h), 250 °C (0.5 h), and 450 °C (12 h). Substantial quantities of a white to yellow solid sublimed onto colder parts of the set-up. The pyrolysis product was a dark brown solid, 0.06 g. Non-condensable volatiles (CH_4), 0.17 mmol, and condensable volatiles (Me_3SiI), 0.91 mmol, were estimated on a calibrated manifold and by IR spectroscopy as for **1** and **2**. Additionally, the titration of the hydrolyzed condensable volatiles provided with 0.91 mmol of Me_3SiI, which was in good agreement with the amount of Me_3SiI obtained from a calibrated manifold. Elemental analysis for the solid product: Ga, 48.79; P, 24.35; Si, 3.75; C, 5.40; H, 0.84 (Σ83.16); Ga/P ratio, 0.89/1.00. IR (cm^{-1}): 803 (w, br), 1042 (s, br), 1742 (w, br). An X-ray diffraction pattern for the product matched the pattern for cubic GaP (JCPDS file 12-191) and a 4.0 nm average particle size was calculated using the Scherrer equation.

Structural analyses of 1-3. Suitable colorless crystals of **1**·C_6H_5Cl, **2**·C_7H_8, and **3** were sealed in glass capillaries under dry argon. A particular crystal was centered on a

diffractometer at a given temperature and determinations of the crystal class, orientation matrix and unit cell parameters were performed. All calculations were performed using the TEXAN[8a] and SHELXTL[8b] structure computer programs. Appropriate neutral atoms scattering factors and their anomalous dispersion corrections were applied.[8c] The structures were solved by direct methods. The non-hydrogen atoms were refined anisotropically. Hydrogen atoms were placed in idealized locations using a standard riding model. Details of the data collection for **1**•C_6H_5Cl, **2**•C_7H_8, and **3** are summarized in Table 1 and Table 2 contains selected bond distances and angles. For **1**•C_6H_5Cl, a total of 3553 unique reflections were collected at 153 K and a total of 2685 reflections were observed ($I > 3\ \sigma(I)$) and used in the final refinement. Full-matrix least-squares methods were used and converged with final residual values of R = 6.58 %, R_w = 8.68 %, and a goodness of fit of 4.19. As **1**•C_6H_5Cl crystallizes in a polar space group, refinement of the model corresponding to the opposite absolute direction of the polar c-axis was also carried out, resulting in final residual values of R = 6.74 %, R_w = 8.82, and a goodness of fit of 4.25. An ORTEP diagram of **1** (the solvent molecule and hydrogen atoms are omitted for clarity) is presented in Figure 3. For **2**•C_7H_8, a total of 4949 unique reflections were collected at 295 K and a total of 1498 reflections were observed ($I > 3\ \sigma(I)$) and used in the final refinement. Full-matrix least-squares methods were utilized and converged with final residual values of R = 4.27%, R_w = 4.65%, and a goodness of fit of 1.35. For **3**, a total of 4007 reflections were collected at 298 K and a total of 3116 independent reflections were used in the final refinement. Full-matrix least-squares methods were applied and converged at ($I > 2\ \sigma(I)$) R = 6.29%, $R(wF^2)$ = 15.42%, and a goodness of fit of 0.957. ORTEP views of **2** and **3** are available in the Supplementary Material.

Results and Discussion

The individual adducts, $X_3Ga{\bullet}P(SiMe_3)_3$ [X = Cl(**1**), Br(**2**), I(**3**)], are obtained in high yields from the reaction between the corresponding gallium trihalide and tris(trimethylsilyl)phosphine in hydrocarbon solvents at ambient temperatures. The isolated solid adducts are stable at room temperature under inert atmosphere for several weeks and their saturated toluene solutions are stable for at least several days as followed by NMR spectroscopy. On the other hand, similar reactions performed with a prolonged sonication of the same reaction mixtures lead to the isolation of the dimeric elimination-condensation products $[X_2GaP(SiMe_3)_2]_2$ (X = Cl, Br, I).[4,5]

^1H and $^{13}C\{^1H\}$ NMR for **1-3** yield in each case doublets which are assigned, respectively, to the protons and carbons of the P-$SiMe_3$ groups. Both the chemical shifts

and coupling constants compare favorably with available NMR data obtained in our laboratory for related organogallium tris(trimethylsilyl)phosphine adducts.[9] The adduct structures of **1-3** are further confirmed by mass spectrometry; the parent ions for the adducts are not detected, but both the ions for GaX_3 and $P(SiMe_3)_3$ are found. The definitive proof of the molecular structures of **1-3** in the solid state is provided by the single-crystal X-ray structure determinations.

As an example, an ORTEP diagram for **1** (the solvent molecule and hydrogen atoms are omitted for clarity) is shown in Figure 3. All three compounds have similar molecular structures with the ligands on the distorted tetrahedral Ga and P centers in a staggered configuration that minimizes steric interactions. The comparison of the Si-P-Si, X-Ga-X, Si-P-Ga, and X-Ga-P angles shows no significant disorder within the $P(SiMe_3)_3$ and GaX_3 fragments for **1**•C_6H_5Cl and **2**•C_7H_8, whereas, for **3** these angles are not uniform and indicate some ligand strain. For example, for **1**•C_6H_5Cl all Cl-Ga-Cl angles are in the 108.3 to 109.9 ° range, for **2**•C_7H_8 the Br-Ga-Br angles are in the 108.5 to 109.6 ° range, but for **3** the I-Ga-I angles are in a significantly wider 109.2 to 115.5 ° range. It is interesting to note that similar trends are observed for other relevant angles in these molecules. Since **1** and **2** crystallize with solvent molecules in the unit cell and **3** is unsolvated in the solid state, it is difficult to directly ascertain the origin of the ligand strain. The Ga-P bond distances for **1**•C_6H_5Cl, 2.380(5) Å (average); **2**•C_7H_8, 2.362(4) Å; and **3**, 2.347(4) Å are similar to each other, and a slight shortening of this bond is observed as the halide bulk increases. This trend seems to be undisturbed by the solvation and crystal packing forces and may reflect a stronger Lewis acidity of the heavier gallium halides. The Ga-P bond lengths in **1**•C_6H_5Cl, **2**•C_7H_8, and **3** can be compared with the few crystallographically characterized 1:1 Ga-P adducts, i.e. Cl_3Ga•PMe_3,[10] $Me_2(Cl)Ga$•$PPh_2CH_2PPh_2$,[11] $(Me_3CCH_2)_3Ga$•$P(H)Ph_2$,[12] Ph_3Ga•$P(SiMe_3)_3$,[13] $Ph_2(Cl)Ga$•$P(SiMe_3)_3$,[13] I_3Ga•PPh_3,[14] and $(Me_3SiCH_2)_3Ga$•$P(SiMe_3)_3$.[9b] The known Ga-P dative bond lengths range from 2.353(2) Å in Cl_3Ga•PMe_3 to 2.6853(5) Å in $(Me_3CCH_2)_3Ga$•$P(H)Ph_2$. The Ga-P distances reported here are rather short, with the one for **3** being the shortest among this family of adducts.

As mentioned above, **1** and **2** are found to be solvated in the solid state. There are two major differences in the packing of the two compounds. In the bromo-derivative, **2**•C_7H_8, the molecules are loosely stacked along the a-axis, with adjacent molecules in the stack being related by the a-glide perpendicular to the c-axis. In the chloro-derivative, **1**•C_6H_5Cl, the two unique molecules in the asymmetric unit also stack along the a-axis in a similar fashion, but rather than an a-glide relationship, they are related by pseudo-translational symmetry. The $GaCl_3$ moieties of **1**•C_6H_5Cl in the stack (and, in fact, in the

whole crystal) point toward the same end of the polar c-axis (as do the C-Cl vectors of the chlorobenzene solvent molecules) rather than alternating back and forth as do the $GaBr_3$ moieties in **2**•C_7H_8. The second difference may be related to the first: the chlorobenzene solvent molecules in **1**•C_6H_5Cl are ordered, rather than disordered, as are the toluene solvent molecules in **2**•C_7H_8. Although there is no obvious reason for the differences in packing of these two compounds, it is presumably due to the difference in size of the halide groups; the larger size of the bromo-groups requiring an alternating stack of molecules. However, the ordered nature of the chlorobenzene solvent molecule may contribute to the observed differences as well.

The efficient formation of these X_3Ga•$P(SiMe_3)_3$ adducts under ambient conditions can be compared with the formation of the appropriate elimination-condensation compounds, $[X_2GaP(SiMe_3)_2]_2$, also reported by us.[4,5] The latter were obtained after prolonged sonication of the respective reaction mixtures in hydrocarbon or hydrocarbon/toluene solvents containing GaX_3 and $P(SiMe_3)_3$. The sonication helped to homogenize the reaction slurries and, at the same time, provided sufficient heat to raise the reaction temperature to about 50 °C. Having isolated the pure adducts **1**, **2**, and **3** we were able to look at this initial elimination chemistry in more detail. For example, a 40 h reflux of the hexane slurry of **1** was as efficient, from the point of view of its conversion to the dimer, as a 14 h sonication followed by a 24 h reflux. However, a closer look at the NMR data for both the adducts and the related dimers made us correct some of our previous proposals regarding the degree of oligomerization of the dimers in the solution.[4,5] We had proposed that the molecules, which are dimers in the solid state, exist in solution as an equilibrium mixture of the monomeric and dimeric species based on the presence of a doublet and a triplet in the proton NMR spectra for the P-$SiMe_3$ groups.[4,5] The doublet was assigned to the monomer and the triplet was thought to result from virtual coupling between the two phosphorus atoms in the dimer. Upon investigating the adduct systems, we noticed that the doublets for the P-$SiMe_3$ protons in the adducts matched the doublets that were first reported for the respective $[X_2GaP(SiMe_3)_2]_2$ dimers and were assigned to the equilibrated monomeric species. It therefore appeared possible that, in our initial NMR studies, instead of monomer-dimer equilibrium of $X_2GaP(SiMe_3)_2$ units we actually had mixtures of unconverted adducts and dimers (because those NMR samples were made from reaction mixtures that were sonicated for short periods of time). Other original characterization data for the dimers (volatiles, EA, MS) were acquired for the recrystallized, pure samples and satisfactorily matched their expected values. In order to further verify this assumption, we prepared a series of NMR samples (in d_8-toluene) of reaction mixtures of $GaCl_3$ and $P(SiMe_3)_3$ after increased sonication times. We observed that the longer the

sonication time, the higher was the proportion of the integrated triplet to doublet in the proton spectra, and no apparent equilibration was taking place. This suggested an irreversible conversion of the adduct $Cl_3Ga{\cdot}P(SiMe_3)_3$ (doublet for P-$SiMe_3$ protons) to the dimer $[Cl_2GaP(SiMe_3)_2]_2$ (triplet for P-$SiMe_3$ protons). As stated above, a 40 h reflux in hexane enabled us to fully convert the adduct. The proton NMR spectrum of a sample of the dimer showed only a stable triplet and no sign of equilibration with other species. Again, this supported the irreversible, one step elimination-condensation chemistry with the formation of a stable dimer. Finally, a variable-temperature ^1H NMR study using a d_8-toluene solution of the pure dimer showed exclusively the triplet at room temperature. The triplet persisted up to 80 °C and no other resonances appeared. At 90 °C, the triplet broadened to a single resonance, most likely due to fast exchange processes at this temperature. Upon cooling, the triplet emerged again and remained unchanged at room temperature for several days. This added credence to our revised proposal of the irreversible conversion of the adduct to the dimer, with the latter existing in solution exclusively as a dimeric species on the NMR time scale. Although no such extensive NMR studies were done for $[Br_2GaP(SiMe_3)_2]_2$ and $[I_2GaP(SiMe_3)_2]_2$, occasional ^1H NMR checks were obtained for samples of reaction mixtures containing GaX_3 (X = Br, I) and $P(SiMe_3)_3$ that were sonicated (or heated) for various times. The ratio of the integrated triplet to the doublet was found to increase irreversibly with reaction time, and no equilibration was detected, as in the case of $[Cl_2GaP(SiMe_3)_2]_2$. All of these observations were consistent with the elimination-condensation chemistry and similar chemical behavior of all three adducts.

The thermogravimetric plots for **1**-**3** are shown in Figure 1. These plots are qualitatively similar in that they all display roughly a three stage weight loss up to 500 °C. The first two stages appear to be superimposed and, quantitatively, they correspond closely to the elimination of two Me_3SiX equivalents from the adduct molecule. The third stage is associated with a smaller relative weight loss and encompasses a wider temperature range. This behavior indicates an incomplete elimination of the residual Me_3SiX groups in all three cases.

All three adducts were pyrolyzed under similar conditions (450 °C, vacuum, analysis of volatiles by IR spectroscopy) to investigate closely their thermal properties. In all cases, based on XRD characterization and elemental analysis, cubic GaP was found to be the major pyrolysis product. The average particle sizes of GaP derived from the respective XRD spectra were 5.0 nm for **1**, 4.6 nm for **2**, and 4.0 nm for **3.** For the pyrolysis of **2,** a TEM micrograph was obtained for the solid product, together with an electron diffraction pattern (Figure 2). The photograph showed crystalline, nanosized

particles of GaP and the diffuse ring diffraction pattern was indexed as belonging to cubic GaP. Additionally, a TEM derived distance between the lattice fringes (3.14 Å) matched well with the known distance between the (111) planes of cubic GaP.

The yields of the crude products, calculated on the basis of pure GaP were 71%, 79%, and 60% for the pyrolysis of **1**, **2**, and **3**, respectively. These relatively high yields reflect the existence of two inherent mass phenomena. First, some intermediate, volatile solids sublimed from the bulk of the pyrolyzed materials under applied conditions - a fact that precluded accurate mass balance determinations. Especially large quantities of the sublimate were observed in the pyrolysis of **3** which could partly explain the low yield in that case. The second phenomenon was associated with a detection of small quantities of methane in the pyrolysis off-gases which, presumably, resulted from thermal cracking of residual trimethylsilyl groups.

The difficulty in removing residual trimethylsilyl groups during the pyrolysis of various $SiMe_3$-containing precursors is well documented and results in the formation of a range of 13-15 composite materials.[2] Such a side-reaction will cause the retention of some silicon, carbon and, possibly, halide in the solid phase and influence mass balance considerations. The elemental analyses of the solid pyrolysis products confirmed the retention of some carbon (**1** - 4.47%, **2** - 0.73%, **3** - 5.40%) and the analysis for silicon in the product from the pyrolysis of **3** gave a Si content of 3.75%, in agreement with the above deductions. Also, the available IR spectra of the solid products from the pyrolyses of **2** and **3** showed two broad bands around 800 cm^{-1} and 1040-1080 cm^{-1} that are typical for Si-C and Si-CH_2-Si moieties,[15] respectively. These likely resulted from the thermal decomposition of the residual $SiMe_3$ groups accompanied by methane evolution. The {Si-C-(H)} species formed an amorphous phase separate from the crystalline GaP under applied conditions. If one compares the outcome of the TGA experiments (small scale, nitrogen flow, uniform heating) with the pyrolysis experiments (larger scale, vacuum, stepwise heating), the significance of the heating conditions on the quantity and, possibly, quality of the final products is quite apparent. Especially important are the limiting conditions of methane formation. In one of the pyrolysis experiments for **1**, the gases evolved on heating the precursor to 300 °C contained CH_4 in addition to Me_3SiCl. Similar observations of methane evolution were noted for the pyrolysis of $[(Me_3Si)_2AlNH_2]_2$,[16a] in which case the onset of CH_4 formation was found at around 200 °C;[16b] additionally, a significant hydrogen evolution commenced at about 600 °C. This suggests that the solid-state bound $SiMe_3$ groups may begin to decompose at temperatures as low as 200 °C. In order to minimize this side-reaction, heating schemes should be devised to remove as much Me_3SiX as possible below this temperature before the formation of non-volatile Si/C

phases takes place. However, complete removal of the Me_3SiX species might be difficult and the retention of some Si, C, H, and X in the final solid product could well be an intrinsic property of these precursor systems. In such a case, appropriate methods of the separation of crystalline 13-15 compounds from amorphous Si/C phases must be developed if high purity materials are to be made.

Acknowledgment. We wish to thank the Air Force Office of Scientific Research, the Office of Naval Research, the AT&T Bell Laboratories Cooperative Research Fellowship Program, and the Duke Endowment Graduate Fellowship Program for their financial support.

Supporting Information Available. ORTEP diagrams for **2** and **3**; tables of bond distances and bond angles, anisotropic temperature factor parameters, and atomic fractional coordinates for **1-3** (21 pages). Ordering information is given on any current masthead page.

References

(1) See for example the following: (a) Mole, T.; Jeffery, E. A. *"Organoaluminum Chemistry"* Elsevier, New York, 1972. (b) *"Chemistry of Aluminum, Gallium, Indium, and Thallium"* Downs, A. J. - Ed., Blackie-Chapman Hall, London, 1993. (c) Neumayer, D. A.; Ekerdt, J. G. *Chem. Mater.* **1996**, *8*, 9. (d) Wells, R. L. *Coord. Chem. Rev.* **1992**, *112*, 273. (e) Paine, R. T.; Narula, C. K. *Chem. Rev.* **1990**, *90*, 73. (f) Cowley, A. H.; Jones, R. A. *Angew. Chem. Int. Ed. Engl.* **1989**, *28*, 1209.

(2) (a) Paine, R. T.; Janik, J. F.; Fan, M. *Polyhedron* **1994**, *13*, 1225. (b) Sauls, F. C.; Hurley, W. J.; Interrante, L. V.; Marchetti, P. S.; Maciel, G. E. *Chem. Mater.* **1995**, *7*, 1361. (c) Paciorek, K. J. L.; Nakahara, J. H.; Hoferkamp, L. A.; George, C.; Flippen-Anderson, J. L.; Gilardi, R.; Schmidt, W. R. *Chem. Mater.* **1991**, *3*, 82. (d) Bender, B. A.; Rice, R.; Spann, J. R. L. *Ceram. Eng. Sci. Proc.* **1985**, *6*, 1171. (e) Izaki, K.; Hakkei, K.; Kawakami, T.; Niimara, K. *"Ultrastructure Processing of Advanced Materials"*, MacKenzie, J. D.; Ulrich, D. R. - Eds., Wiley, New York, 1988, 891. (f) Baixia, L.; Yinkui, L.; Yi, L. *J. Mater. Chem.* **1993**, *3*, 117.

(3) Kher, S. S.; Wells, R. L. *Chem. Mater.* **1994**, *6*, 2056.

(4) Wells, R. L.; Self, M. F.; McPhail, A. T.; Aubuchon, S. R.; Woudenberg, R. C.; Jasinski, J. P. *Organometallics* **1993**, *12*, 2832.

(5) (a) Aubuchon, S. R.; McPhail, A. T.; Wells, R. L.; Giambra, J. A.; Bowser, J. R. *Chem. Mater.* **1994**, *6*, 82. (b) Wells, R. L.; Aubuchon, S. R., Lube, M. S. *Main Group Chemistry* **1995**, *1*, 81.

(6) Shriver, D. F.; Drezdzon, M. A. *"The Manipulation of Air Sensitive Compounds"* Wiley-Interscience, New York, 1986.

(7) Becker, G.; Hölderich, W. *Chem. Ber.* **1975**, *108*, 2484.

(8) (a) Swepston, P. N. *"TEXAN; Structure Analysis Software"*, Molecular Structure Corporation, The Woodlands, Texas, 1993; (b) Sheldrick, G. M. *"SHELXTL, Crystallographic Computing System"*, Nicolet Instruments Division: Madison, WI, 1986.

(c) *"International Tables for X-ray Crystallography"*, The Kynoch Press, Birmingham, England, 1974.

(9) (a) Wells, R. L.; Aubuchon, S. R.; Self, M. F.; Jasinski, J. P.; Woudenberg, R. C.; Butcher, R. J. *Organometallics* **1992**, *11*, 3370. (b) Wells, R. L.; Baldwin, R. A.; White, P. S. *Organometallics* **1995**, *14*, 2123.

(10) Carter, J.; Jugie, G.; Enjalbert, R.; Galy, J. *Inorg. Chem.* **1978**, *17*, 1248.

(11) Schmidbaur, H.; Lauteschlager, S.; Müller, G. *J. Organomet. Chem.* **1985**, *281*, 25.

(12) Banks, M. A.; Beachley, O.T., Jr.; Maloney, J. D. *Polyhedron* **1990**, *9*, 335.

(13) Wells, R. L.; Aubuchon, S. R.; Self, M. F.; Jasinski, J. P.; Woudenberg, R. C.; Butcher, R. J. *Organometallics* **1992**, *11*, 3370.

(14) Taylor, M. J.; *private communication*, **1994**.

(15) Schmidt, W. R.; Interrante, L. V.; Doremus, R. H.; Trout, T. K.; Marchetti, P. S.; Maciel, G. E. *Chem. Mater.* **1991**, *3*, 257.

(16) (a) Janik, J. F.; Duesler, E. N.; Paine, R. T. *Inorg. Chem.* **1987**, *26*, 4341. (b) Janik, J. F. *"Investigation of Group III-V Compounds as Precursors for Solid State Materials"*, Ph.D. Dissertation, University of New Mexico, USA, 1987.

Captions to Figures

Figure 1. Thermogravimetric analysis (TGA) data for the decomposition of: $Cl_3Ga{\bullet}P(SiMe_3)_3$ (**1**), curve **A**; $Br_3Ga{\bullet}P(SiMe_3)_3$ (**2**), curve **B**; $I_3Ga{\bullet}P(SiMe_3)_3$ (**3**), curve **C**.

Figure 2. Transmission electron micrograph (TEM) image and electron diffraction ring pattern for GaP powder derived from the pyrolysis of $Br_3Ga{\bullet}P(SiMe_3)_3$ (**2**).

Figure 3. ORTEP diagram (35% probability ellipsoids) showing the solid-state structure and atom numbering scheme of **1**. The solvent molecule and hydrogen atoms are omitted for clarity.

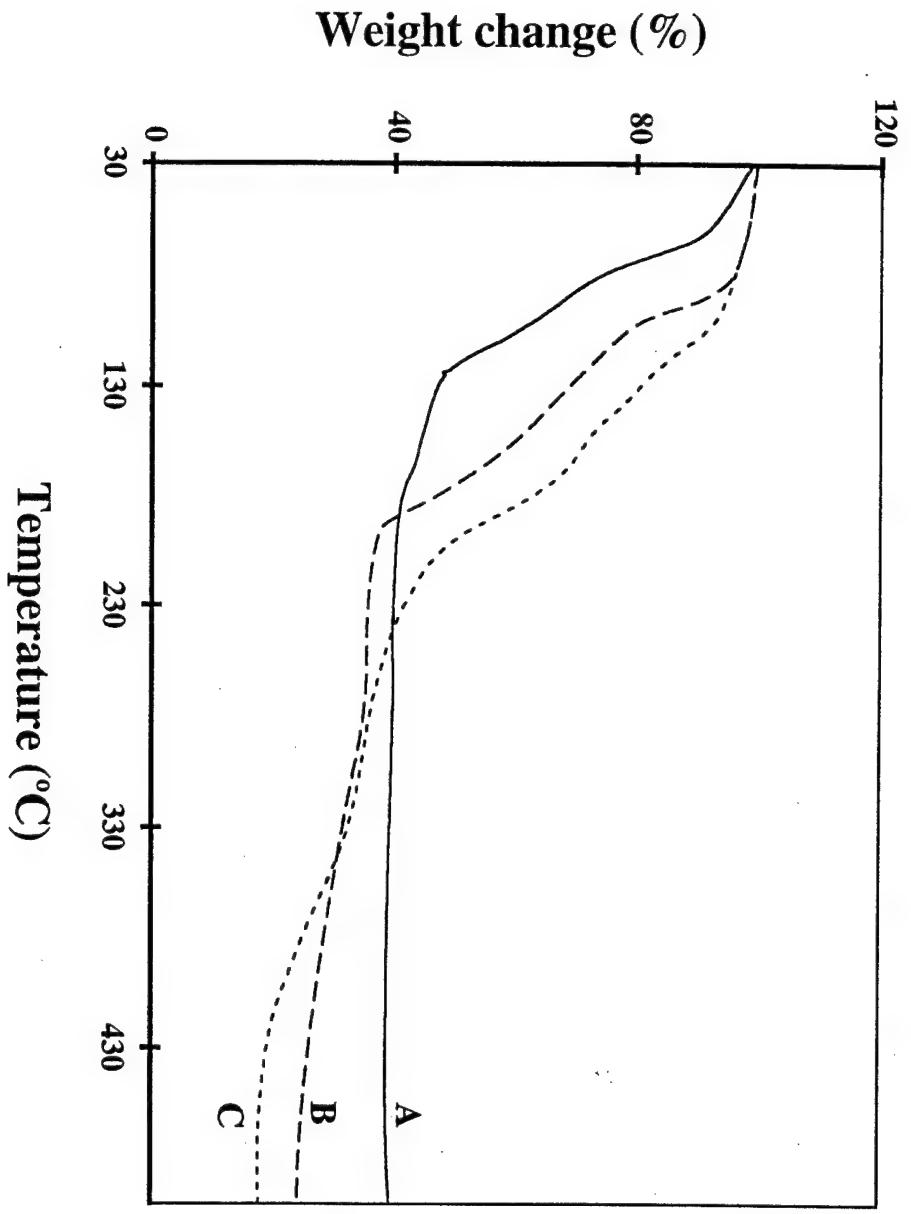

Figure 1

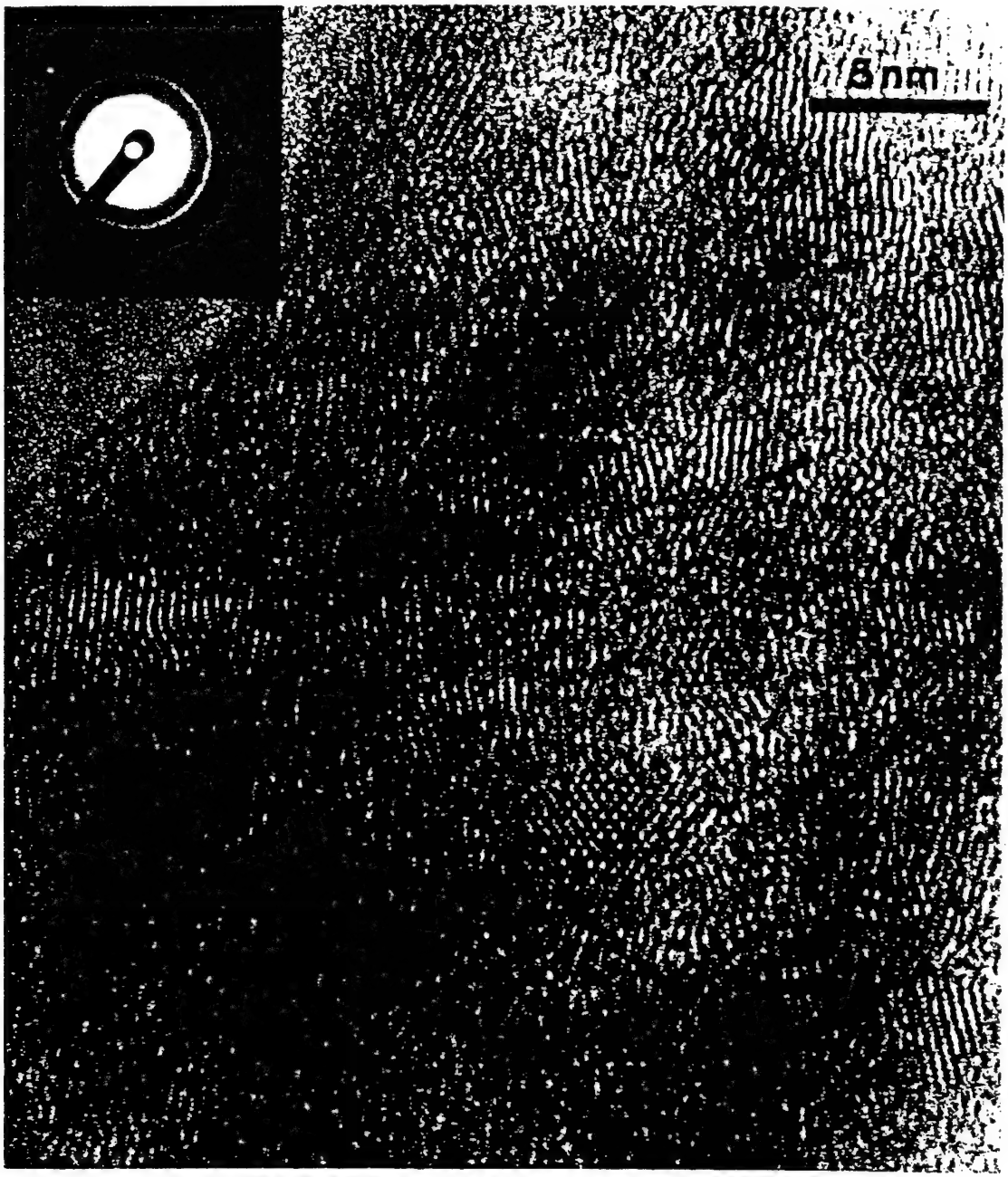

Figure 2

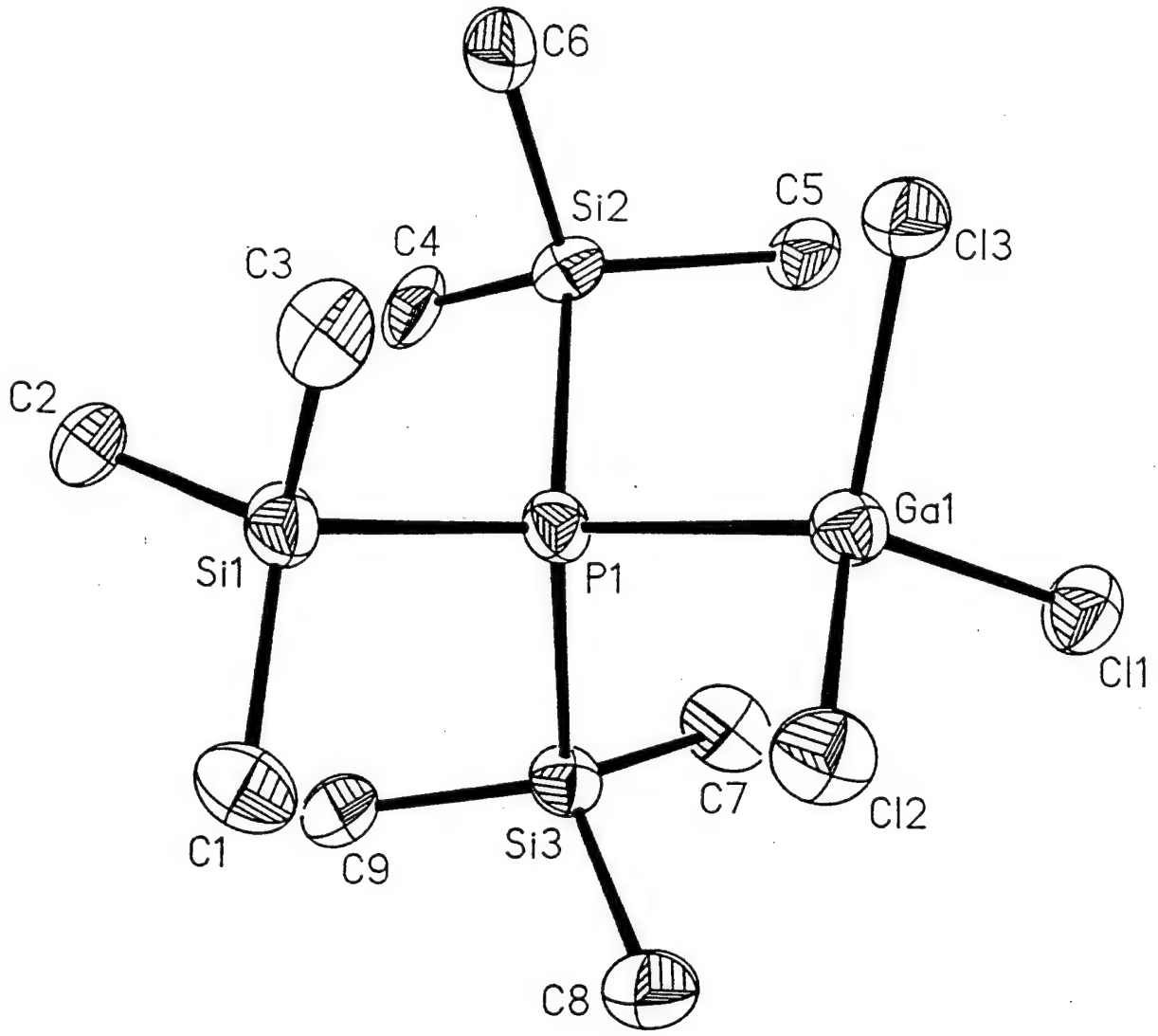

Figure 3

Table 1. Crystallographic Data and Measurements for **1**•C_6H_5Cl, **2**•C_7H_8, and **3**.

	1•C_6H_5Cl	**2**•C_7H_8	**3**
molecular formula	$C_{15}H_{32}GaCl_4PSi_3$	$C_{16}H_{35}GaBr_3PSi_3$	$C_9H_{27}GaI_3PSi_3$
formula weight	539.17	652.13	700.97
crystal system	orthorhombic	orthorhombic	monoclinic
space group	$Pbc2_1$[a]	Pbca	$P2_1/c$
a, Å	17.270(4)	17.679(5)	16.336(2)
b, Å	22.054(5)	22.756(5)	9.590(1)
c, Å	13.550(4)	13.966(4)	16.485(1)
β, deg	90.000(-)	90.000(-)	112.733(9)
V, Å^3	5161(2)	5618(2)	2381.9(5)
Z	8	8	4
radiation (wavelength, Å)	Mo-Kα (0.71073)	Mo-Kα (0.71073)	Mo-Kα (0.71073)
μ, cm^{-1}	16.8	54.3	52.5
temp, °C	-120	22	25
D_{calcd}, g cm^{-3}	1.388	1.542	1.955
crystal dimens., mm	0.23 x 0.25 x 0.35	0.16 x 0.22 x 0.31	0.40 x 0.40 x 0.08
T_{max}; T_{min}	1.00:0.58	1.00:0.81	0.61:0.33
scan type	ω/2Θ	ω/2Θ	ω
$2\Theta_{max}$, deg	50	50	45
no. of rflns recorded	3553	4949	4007

Table 1 (continued)

	1	**2**	**3**
no. of non-equiv. rflns recorded	3553	4949	3119
no. of rflns retained, $I > 2.0\sigma(I)$ or $I > 3.0\sigma(I)$	2685	1498	3116
no. of params. refined	433	195	252
$R(F)^b$; $R_w{}^c$ or $R(wF^2)^d$	0.066^b; 0.087^c	0.043^b; 0.046^c	0.063^b; 0.154^d
goodness-of-fit[e]	4.19	1.35	0.957
max shift / esd. in final least-squares cycle	0.004	0.004	0.081
final max, min $\Delta\rho$, e/Å^{-3}	1.02; -0.90	0.63; -0.40	1.24; -1.26

[a] The non-standard setting of space group $Pca2_1$ (No. 29) was chosen to facilitate comparison to the similar crystal packing and metric parameters of compound **2**•C_7H_8.

[b] $R(F) = \Sigma(||F_o| - |F_c||)/\Sigma|F_o|$

[c] $R_w = [\Sigma w(|F_o| - |F_c|)^2/\Sigma w|F_o|^2]^{1/2}$

[d] $R(wF^2) = \Sigma[w(F_o^2 - F_c^2)^2]/\Sigma[(wF_o^2)^2]^{1/2}$

[e] Goodness-of-fit = $[\Sigma w\Delta^2/(N_{observations} - N_{parameters})]^{1/2}$.

Table 2. Selected bond distances (Å) and angles (°) for **1**•C_6H_5Cl, **2**•C_7H_8, and **3** with Estimated Standard Deviations in Parentheses

	Bond Lengths		
	1	**2**	**3**
Ga(1)-P(1)	2.379(5)	2.362(4)	2.347(4)
Ga(2)-P(2)	2.380(5)	----	----
P(1)-Si(1)	2.306(7)	2.308(5)	2.39(1)
P(2)-Si(4)	2.295(7)	----	----
Ga(1)-Cl(1)	2.169(4)	----	----
Ga(2)-Cl(2)	2.176(4)	----	----
Ga-Br(1)	----	2.315(2)	----
Ga-I(1)	----	----	2.564(2)
Si(1)-C(1)	1.83(2)	1.84(1)	2.07(5)
Si(4)-C(10)	1.87(2)	----	----
	Bond Angles		
	1	**2**	**3**
Cl(1)-Ga(1)-Cl(2)	109.4(2)	----	----
Br(1)-Ga(1)-Br(2)	----	108.7(1)	----
I(1)-Ga(1)-I(2)	----	----	109.15(7)
I(2)-Ga(1)-I(3)	----	----	115(49)(13)
Cl(1)-Ga(1)-P(1)	110.4(2)	----	----
Br(1)-Ga(1)-P(1)	----	110.3(1)	----
I(1)-Ga(1)-P(1)	----	----	109.23(13)
Ga(1)-P(1)-Si(1)	107.8(2)	108.8(2)	103.0(4)
Si(1)-P(1)-Si(2)	111.3(3)	110.0(2)	102.3(6)

TECHNICAL REPORTS DISTRIBUTION LIST

ORGANOMETALLIC CHEMISTRY FOR ELECTRONIC & OPTICAL MATERIALS

Dr. Harold E. Guard
Code 1113
Chemistry Division, 331
Office of Naval Research
800 N. Quincy Street
Arlington, Va 22217-5660

Dr. Richard W. Drisko
Naval Facilities & Engineering
Service Center
Code L52
Port Hueneme, CA 93043

Defense Technical Information
Center
Building 5, Cameron Station
Alexandria, VA 22314

Dr. Eugene C. Fischer
Code 2840
Naval Surface Warfare Center
Carderock Division Detachment
Annapolis, MD 21402-1198

Dr. James S. Murday
Chemistry Division, Code 6100
Naval Research Laboratory
Washington, DC 20375-5320

Dr. Bernard E. Douda
Crane Division
Naval Surface Warfare Center
Crane, IN 47522-5000

Dr. John Fischer, Director
Chemistry Division, C0235
Naval Air Weapons Center
Weapons Division
China Lake, CA 93555-6001

Dr. Peter Seligman
Naval Command, Control and
Ocean Surveillance Center
RDT&E Division
San Diego, CA 93152-5000